



Comparison of the plastic hinge deformation limits between ASCE 41 and CSA S6-14 for the retrofit of existing reinforced concrete bridges Case Study of Agassiz-Rosedale Bridge

Sepideh Ashtari¹, Thierry Chicoine², Jianping Jiang³, Carlos Ventura⁴

¹ Ph.D., EIT, Designer, Bridges, WSP Canada, Vancouver, BC, Canada.

² Ph.D., P.Eng., Senior Bridge Engineer, WSP Canada, Vancouver, BC, Canada.

³ Ph.D., P.Eng., National Practice Leader for Bridges & Civil Structures, WSP Canada, Vancouver, BC, Canada.

⁴ Professor and Director of Earthquake Engineering Research Facility, Department of Civil Engineering, University of British Columbia, Vancouver, BC, Canada

ABSTRACT

This paper aims to provide a comparison of deformation limits in plastic hinges of existing reinforced concrete bridge pier columns, by comparing the methods presented in ASCE 41 using plastic hinge rotation limits and the strain limits of CSA S6-14 and the BC Ministry of Transportation and Infrastructure (BC MoTI) Supplement. As a case study, the seismic performance of one short pier and one tall pier from the Agassiz-Rosedale Bridge were evaluated using different plastic hinge behaviours. Different hinge behaviours from ASCE 41 were considered to represent different possible modes of failure in the bridge columns. The strains corresponding to the ultimate hinge limits were post-processed after the pushover analysis of the piers and were compared to the CSA S6-14 and BC MoTI Supplement strain limits. For the nonlinear pushover analysis models, the effects of upper-bound and lower-bound plastic hinge lengths were investigated. The comparison of the strain values suggests that for both tall and short piers, the strain limits in the plastic hinges corresponding to the ultimate limits of ASCE 41 are much smaller than those derived from CSA S6-14 and the BC MoTI supplement. The deformation limits from both codes are considerably sensitive to the assumed plastic hinge length, which depends on the height of the pier and the equations used to estimate it.

Keywords: seismic retrofit, bridges, ASCE 41, CSA S6-14, deformation limits.

INTRODUCTION

The 2014 edition of the Canadian Highway Bridge Design Code, CSA S6-14, adopted for the first time a performance-based approach for the seismic design of new bridges and retrofit design of existing bridges. The CSA S6-14 performance-based approach prescribes minimum structural performance levels at three hazard levels with 2%, 5%, and 10% probabilities of exceedance in 50 years, corresponding to return periods of 2475, 975, and 475-year, respectively. For each performance level, performance criteria were specified in terms of acceptable structural damage and expected serviceability. For reinforced concrete structures, the structural performance criteria were defined in terms of strain limits of reinforcing steel and concrete. The CSA S6-14 performance levels and the associated strain limits for reinforced concrete bridges are summarized in Table 1. The associated strain limits were found to be unduly conservative for the minimal and repairable damage performance levels. Moreover, no strain limits were specified for the probable replacement performance level. As a result, the BC MoTI Supplement to CSA S6-14 adjusted the strain limits associated to each performance levels as summarized in Table 2. A thorough evaluation and comparison of the two sets of performance criteria can be found in Ashtari [1] and Ashtari et al. [2].

For performance-based seismic assessment of existing bridges, both CSA S6-14 and the BC MoTI Supplement employ the same set of strain limits associated to the minimal damage performance level as for new bridges. The seismic behaviour of older existing bridges with obsolete structural details, however, is very different than for new bridges and the current code strain limits may not be appropriate for their assessment. It is not clear at this point whether the recommended strain limits for new bridges would result in the same expected performance levels in existing bridges. Recently some new revisions were suggested to address this issue in the public review draft of CSA S6-19. Therefore, there is a need to calibrate more appropriate strain limits to the expected performance levels of existing bridges.

It is interesting to note that for the seismic evaluation and retrofit design of existing buildings, ASCE 41 addresses this issue by providing component-level backbone curves with limits on plastic rotation or drift ratios. These limits are established based

on the seismic demands and confinement details of a component. It would be interesting to investigate whether the use of ASCE 41 backbone curves can be extended for the assessment of existing bridges. It is especially of interest to understand how the models utilizing ASCE 41 plastic hinges would predict the performance of ductile reinforced concrete bridge columns compared to the models employing the strain limits of CSA S6-14 & BC MoTI Supplement. As a first comparison, the application of both ASCE 41 and CSA S6-14 & BC MoTI Supplement is investigated on the Agassiz-Rosedale Bridge, a lifeline bridge carrying Highway 9 over the Fraser River in British Columbia, Canada.

Table 1. CSA S6-14 strain limits for RC bridges

Damage Level	Concrete Strain	Reinforcing Steel Strain
Minimal	$\epsilon_c > -0.004$	$\epsilon_s < \epsilon_y$
Repairable	Not Defined	$\epsilon_s < 0.015$
Extensive	$\epsilon_{cc} > \epsilon_{cu}$	$\epsilon_s < 0.050$
Probable Replacement	Not Defined	Not Defined

Table 2. BC MoTI Supplement strain limits for RC bridges

Damage Level	Concrete Strain	Reinforcing Steel Strain
Minimal	$\epsilon_c > -0.006$	$\epsilon_s < 0.010$
Repairable	Not Defined	$\epsilon_s < 0.025$
Extensive	$\epsilon_{cc} > 0.8 \epsilon_{cu}$	$\epsilon_s < 0.050$
Probable Replacement	$\epsilon_{cc} > \epsilon_{cu}$	$\epsilon_s < 0.075$ (30 M or smaller) $\epsilon_s < 0.060$ (35 M or larger)

DESCRIPTION OF THE BRIDGE

The Agassiz-Rosedale Bridge (Figure 1) is a lifeline bridge located along Highway 9, crossing the Fraser River just south of Agassiz, BC. The 1.9 km long bridge includes 6 river spans, the South and North Approaches of 11 and 25 spans, respectively, and the North Viaduct of 50 spans. The river spans are composed of steel deck/through truss on reinforced concrete wall-type piers, and the approach and viaduct spans are made up by composite steel-girder concrete deck on reinforced concrete piers. The bridge was selected by the BC Ministry of Transportation and Infrastructure for seismic retrofit and functional upgrade, which includes widening of the bridge superstructure.

Two piers (N2 and N24) from the North Approach spans were selected for this study, which represent the second tallest and shortest piers in the approach spans, respectively. The existing bridge bents are comprised of a cap beam and two rectangular columns on individual pile foundations with H-piles in 2x4 or 3x3 arrangements. The main vertical reinforcing bars are terminated at the base of the pier columns and spliced with dowels coming out of the pile caps. The proposed retrofit measures for the substructure of the North and South approach spans include combining the individual pile foundations into an extended single larger pile foundation, adding new piles underneath the new pile caps, and possible jacketing for columns, as shown in Figure 2. Due to functional upgrade, the cap beams and the deck are widened to accommodate new side walks on each side of the road.



Figure 1. Agassiz-Rosedale Bridge

response of the columns shifts from ductile to limited ductility. Condition iii and iv primarily represent brittle response with limited to no ductility.

The hinge behaviours selected for this study from the Table 10-8 of ASCE 41-13 are listed in Table 4 along with the nonlinear hinge parameters. Figure 3 illustrates the shape of the backbone curves and the hinge parameters corresponding to various conditions listed in the table. The following should be noted:

- 1- The axial force ratio of the approach piers was below 0.1 under service loads, and higher than 0.1 but much lower than 0.6 under the ultimate earthquake load combinations. The hinge parameters at the higher axial load ratio were only used to interpolate the hinge behaviour for the intermediate axial load ratios between 0.1 and 0.6 in the analysis program.
- 2- The shear demand to capacity ratio of the piers were lower than 0.5. It was decided to employ both of the “Low-Shear” (LS) and “High-Shear” (HS) hinge parameters for the columns to investigate the semi-ductile behaviour.
- 3- Condition i is not applicable to the existing columns without any retrofit measures. However, they could be applicable to the case where additional confinement and shear capacity are provided by the retrofit measures (e. g. Steel or FRP jacket).

Table 3. Conditions to be used for columns in Table 10-8 ASCE 41-13

	ACI 318 Conforming Seismic Details with 135 Hooks	Closed Hoops with 90-degree Hooks	Other (Including Lap- Spliced Transverse Reinforcement)
$V_p/V_o \leq 0.6$	i ^a	ii	ii
$1.0 \geq V_p/V_o > 0.6$	ii	ii	iii
$V_p/V_o > 1.0$	iii	iii	iii

^aTo qualify for Condition i, a column should have $A_v/b_w s \geq 0.002$ and $s/d \leq 0.5$ within flexural plastic hinge region, other wise Condition ii should be assigned.

Table 4. Selected hinge behaviours from Table 10-8 ASCE 41-13

	$P/A_g f'_c$	$\rho = A_v/b_w s$	$V/b_w d \sqrt{f'_c}$	Plastic Rotation Limit (rad)		Residual Strength
				a	b	c
Condition i	≤ 0.1	0.002	-	0.027	0.034	0.2
	≥ 0.6	0.002	-	0.005	0.005	0.0
Condition ii	≤ 0.1	≤ 0.0005	≤ 0.25	0.012	0.012	0.2
	≥ 0.6	≤ 0.0005	≤ 0.25	0.004	0.004	0.0
	≤ 0.1	≤ 0.0005	≥ 0.5	0.006	0.006	0.2
	≥ 0.6	≤ 0.0005	≥ 0.5	0.000	0.000	0.0
Condition iii	≤ 0.1	≤ 0.0005	-	0.000	0.006	0.0
	≥ 0.6	≤ 0.0005	-	0.000	0.000	0.0
Condition iv	≤ 0.1	≤ 0.0005	-	0.000	0.006	0.2
	≥ 0.6	≤ 0.0005	-	0.000	0.000	0.0

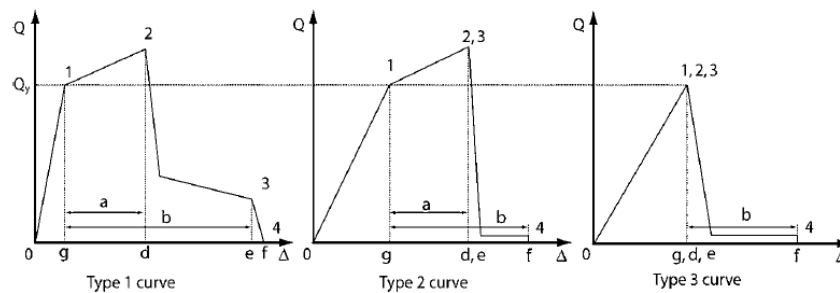


Figure 3. Typical backbone curves and modelling parameters for nonlinear static procedures in ASCE-41

Plastic Hinge Length Expressions

A commonly used expression for estimating the plastic hinge length of reinforced concrete columns (without jackets) is proposed by Priestley et al. [5] and has been adopted in Caltrans SDC 1.7 and WSDOT Bridge Design Manual for new bridges:

$$L_p = \max \text{ of } (0.08 L + 0.022 f_{ye} d_{bl} \text{ and } 0.044 f_{ye} d_{bl}) \text{ (mm, MPa)} \quad (2)$$

Where f_{ye} is the expected yield strength of the reinforcing steel and d_{bl} is the diameter of the longitudinal reinforcing steel.

Priestley et al. also recommended using the lower-bound limit of Equation 2 for calculating the plastic hinge length of poorly confined columns in existing bridges, which are expected to sustain large inelastic rotations in plastic hinges:

$$L_p = \min \text{ of } (0.08 L + 0.022 f_{ye} d_{bl} \text{ and } 0.044 f_{ye} d_{bl}) \text{ (mm, MPa)} \quad (3)$$

It should be noted that $0.022 f_{ye} d_{bl}$ represents strain penetration length, and the lower-bound limit is in fact twice this length to consider strain penetration on both sides of the critical section at plastic hinge. Equation 3 has also been suggested by FHWA Seismic Retrofit Manual for obtaining plastic hinge length with sufficient lap splice length for existing bridges.

Both above equations were employed to estimate the Upper-Bound (UB) and Lower-Bound (LB) plastic hinge length for the selected piers of the Agassiz-Rosedale Bridge.

Obtaining Equivalent Strain Limits for the ASCE 41 Deformation Limits

To obtain the strains corresponding to the ultimate limit of the ASCE 41 plastic hinges in the pushover models, first the plastic curvature at the ultimate limit was calculated by employing the method outlined in Caltrans SDC 3.1.3 and assuming single curvature deformation for the pier columns in the longitudinal earthquake direction. This method relates the global displacement response to the local curvature response of a member. Subsequently, a separate sectional analysis was performed in Response 2000 to find the strain limits corresponding to the obtained plastic curvature.

NUMERICAL MODELS

Individual models of Pier N2 and N24 were generated in the CSI Bridge analysis platform. For each pier, five models were created, corresponding to different hinge behaviours defined in Table 4, as listed below, and assuming lower-bound plastic hinge length from Equation 3:

- Model i (with Condition i hinge)
- Model ii-LS (with Condition ii Low-Shear hinge)
- Model ii-HS (with Condition ii High-Shear hinge)
- Model iii (with Condition iii hinge)
- Model iv (with Condition iv hinge)

For Pier N2, additional models were created using the upper-bound plastic hinge length from Equation 2, to give a perspective on sensitivity of the results to the assumed plastic hinge length. In total 15 numerical models were analyzed, details of which are given next.

Material Properties

The specified compressive strength of concrete was 25 MPa for the existing pile caps and 35 MPa for the existing concrete other than the pile caps. The specified compressive strength of concrete for new components was taken as 35 MPa. The yield strength of the existing and new structural steel for piles was 230 MPa and 310 MPa, respectively. For reinforcing steel, the yield strength was also conservatively taken as 230 MPa for the performance assessment of the columns. The yield strength of the new reinforcing steel was taken as 400 MPa.

Structural Configuration

Each pier consisted of two rectangular columns connected at the top with a deep rectangular cap beam and at the base supported by the combined pile foundation. The dimensions and reinforcing details of the columns and cap beams are summarized in Table 5 and 6. In Table 5, H_1 is the clear height of the column and H_2 is the height from top of the existing pile caps to the middle depth of the cap beam.

Each of two existing pile foundations for N2 was comprised of a concrete pile cap of 6.0 ft wide, 12.0 ft long and 5.0 ft deep, supported by 8 HP12x53 piles, arranged in a 2x4 formation. The pile foundations for N24 had a concrete pile cap of 9.0 ft wide, 9.0 ft long and 4.0 ft deep, supported by 9 HP12x53 piles in a 3x3 arrangement. The enlarged pile caps combined the existing caps into a single cap at each pier with an additional overlay of 0.6 m thick. The additional piles consist of 762 mm diameter

x19 mm thick steel pipe piles filled with reinforced concrete. Two and four new piles were added to Pier N2 and Pier N24, respectively, in the retrofit design. Other details of the foundation and superstructure configuration are dispensable for the sake of this study, and for brevity are not presented.

Table 5. Column dimensions and reinforcing details for Pier N2 and N24

Pier	H_1 (m)	H_2 (m)	L (m)	w (m)	Reinforcement	
					Longitudinal	Transverse
N2	15.27	16.49	1.37	1.22	16-#10	#3 @ 0.152
N24	2.88	3.95	1.22	1.07	12-#10	#3 @ 0.152

Table 6. Cap beam dimensions and reinforcing details for Pier N2 and N24

Pier	Depth (m)	Length(m)	Width (m)	Reinforcement			
				Top	Bot	Sides	Transverse
N2	2.44	9.14	1.22	5-#10	9-#11	2* 4-#4	#4 stirrups in pairs @ 0.610 m
N24	2.13	9.14	1.07	5-#10	9-#11	2* 4-#4	#4 stirrups in pairs @ 0.610 m

Structural Models

A snapshot of the pushover analysis model of Pier N2 is shown in Figure 4, along with the details of the model. For the local pushover analysis of the individual piers, the tributary mass of the superstructure was assigned to the top of the rigid massless frame, which would locate the mass at the center of mass of the superstructure. The tributary dead loads from the superstructure were applied as concentrated loads at the bearing locations to the rigid frame.

The columns were modelled with frame elements having effective flexural, shear, and torsion stiffness. P-M-M interaction hinges with the ASCE 41 backbone curves were assigned to the bottom of the columns at a distance equal to $L_p/2$. Because pushover in the longitudinal direction will cause the columns to deform in single curvature, the plastic hinges would only form at the bottom of the columns.

To model the existing pile caps, thin shell elements were used, while the components connecting the existing pile caps was modelled using beam analogy and a network of frame and link elements, as shown in the figure. The piles were extended in the model to their equivalent depth of fixities, which were taken 2.5 m for the existing H-piles and 4.5 m for the new piles. Bi-linear elastic-perfectly-plastic link elements were incorporated at the ends of the existing H-pile, which would allow redistribution of the loads to the new piles, once the existing piles have reached their load bearing capacities (i.e. 200 kN in tension and 400 kN in compression per pile). Moreover, due to large surface area of the new pile caps, bi-linear passive soil springs were added at the pile cap level in the longitudinal direction to simulate the passive soil pressure. The mass of the pile caps was also included in the analysis.

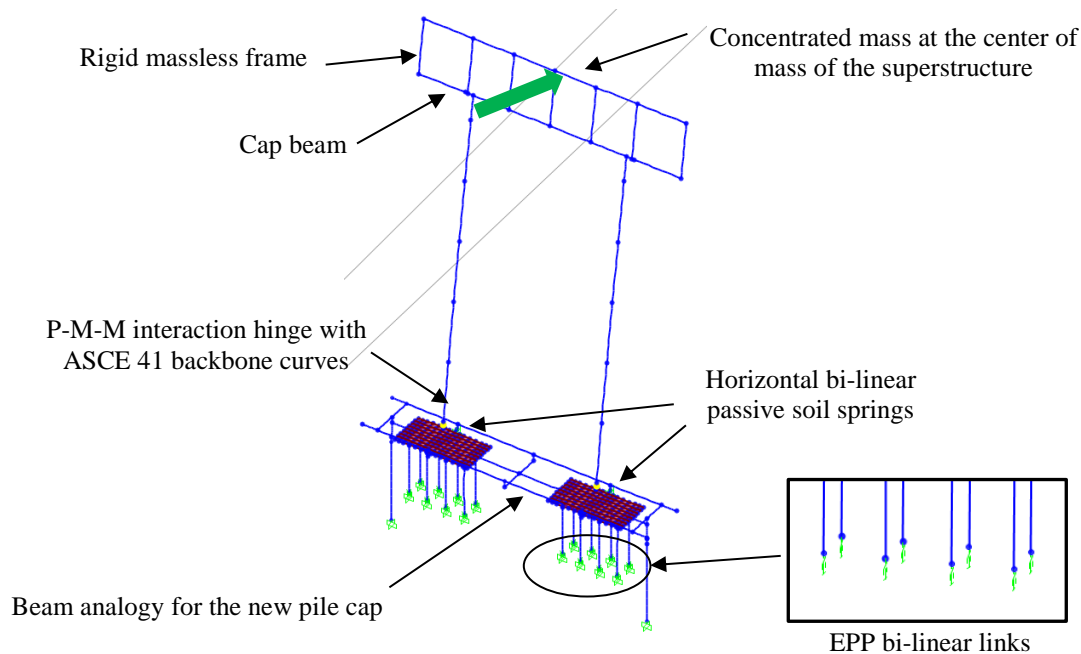


Figure 4. Pushover model of Pier N2

PUSHOVER ANALYSIS

Uni-directional pushover analyses of the individual pier bents were performed. The pier bents were pushed using a displacement-controlled analysis in the longitudinal direction until failure, indicated by the plastic hinges reaching to their ultimate plastic limits or by the inability of analysis to converge beyond that point. The pushover profile was based on the inertial mass distribution automatically calculated by the program.

ANALYSIS RESULTS AND DISCUSSIONS

The pushover curves for the Pier N2 and N24 employing the ASCE 41 plastic hinge behaviours of Table 4 are presented in Figure 5. The curves reveal the drift ratio limits for the failure of the columns assuming different ASCE 41 hinge behaviours. For Condition i, a drift ratio of 3-4% would cause failure. For Condition ii-LS, a drift of 1.5-2% and for Condition ii-HS, a drift of 1.0-1.5% would lead to failure. For condition iii and iv, a drift of only 0.5-1% would lead to collapse. It should be noted that the negative slope in the Pier N2 pushover curves compared to the relatively flat post-yield response of Pier N2, is due to P-delta effects on these tall columns.

The strain limits corresponding to the failure of the plastic hinges are summarized in Table 7, along with the curvature ductility at failure. In this table, ε_c and ε_s are concrete and reinforcing steel strains, φ and φ_e are the curvature and curvature at yielding, and μ_φ is the curvature ductility. Comparing the strain limits obtained from the Pier N2-LB with Pier N24-LB models, shows some discrepancies, which are only prominent for Condition i. Comparing the strain limits of both tables with the CSA S6-14 and BC MoTI Supplement limits (Table 1 and 2), the following can be observed:

- The strain limits for Condition i behaviour, are closer to those from the BC MoTI Supplement corresponding to probable replacement performance level, governed by the reinforcing steel strain limit.
- The strain limits for Condition ii-LS corresponds to strain limits for a performance level between repairable damage and extensive damage in the BC MoTI Supplement.
- The strain limits for Condition ii-HS corresponds to strain limits for a performance level between minimal and repairable damage in CSA S6-14.
- The strain limits for Condition iii and iv, corresponds to a performance level of minimal damage in either CSA S6-14 or BC MoTI Supplement, where some minor reinforcement yielding and minor superficial cover cracking is expected.

Considering that all the obtained strain limits for Conditions i to iv represent initiation of a failure mode, it can be readily observed that the current strain limits of CSA S6-14 and BC MoTI Supplement do not necessarily lead to the expected performance levels of existing RC bridges as defined for new bridges, except when flexural failure is expected in an existing bridge. For instance, for a modern RC bridge column, a compressive strain limit of -0.005 in concrete may correspond to minor spalling and minimal damage performance level, while in an existing RC bridge where shear-flexure mode of failure is dominant, it may lead to extensive damage or failure.

Another important insight is gained by comparing the strain limits obtained from the Pier N2 models with upper-bound and lower-bound plastic hinge lengths. The comparison reveals that the obtained strain limits are highly sensitive to the assumed plastic hinge length. Therefore, utilizing appropriate plastic hinge length expression is very critical to the outcome of the performance evaluation. Currently, CSA S6-14 and BC MoTI Supplement do not provide specific recommendations on this matter.

Based on the above observations, the following recommendations are proposed for future editions of CSA S6:

1. It is necessary to provide a separate set of performance criteria and performance levels for the evaluation of existing bridges. It would be important for the code to define the expected performance levels based on the expected modes of failure, including flexure, shear-flexure, shear, and lap-splice failure, and then associate appropriate strain limits to each level.
2. The code should highlight the importance of employing appropriate plastic hinge length in seismic performance evaluation, and should provide specific guidance in the code commentary. A sensitivity analysis is recommended using the upper-bound and lower-bound plastic hinge lengths to verify the performance.

CONCLUSIONS

The strain limits in the plastic hinges corresponding to the ultimate rotation limits of the ASCE 41 were compared against the strain limits prescribed in CSA S6-14 and the BC MoTI Supplement. Recommendations were provided regarding calibrating appropriate strain limits to expected performance levels for existing RC bridges for considerations in future editions of CSA S6.

REFERENCES

- [1] Ashtari, S. (2018). *Evaluating the performance-based seismic design of RC bridges according to the 2014 Canadian Highway Bridge Design Code*. PhD Dissertation, University of British Columbia, Vancouver, BC.
- [2] Ashtari, S., Ventura, C., Finn, W. D. L., Kennedy, D. (2017). "A case study on evaluating the performance criteria of the 2014 Canadian Highway Bridge Design Code." In 39th IABSE Symposium, Vancouver, BC.
- [3] Elwood, K.J., Matamoros, A.B., Wallace, J.W., Lehman, D.E., Heintza, J.A., Mitchell, A.D.; Moore, M.A., Valley, M.T., Lowes, L.N., Comartin, C.D., Moehle, J.P. (2007). "Update to ASCE/SEI 41 concrete provisions," *Earthquake Spectra*, 23(3), 493-523
- [4] Cho, J., Pincheira, J.A. (2006). "Inelastic analysis of reinforced concrete columns with short lap splices subjected to reversed cyclic loads," *ACI Structural Journal*, 103(2), 280-290.
- [5] Priestley, M.J.N, Seisble, F., Calvi, G.M. (1996). *Seismic Design and Retrofit of Bridges*. John Wiley and Sons, Inc., US.

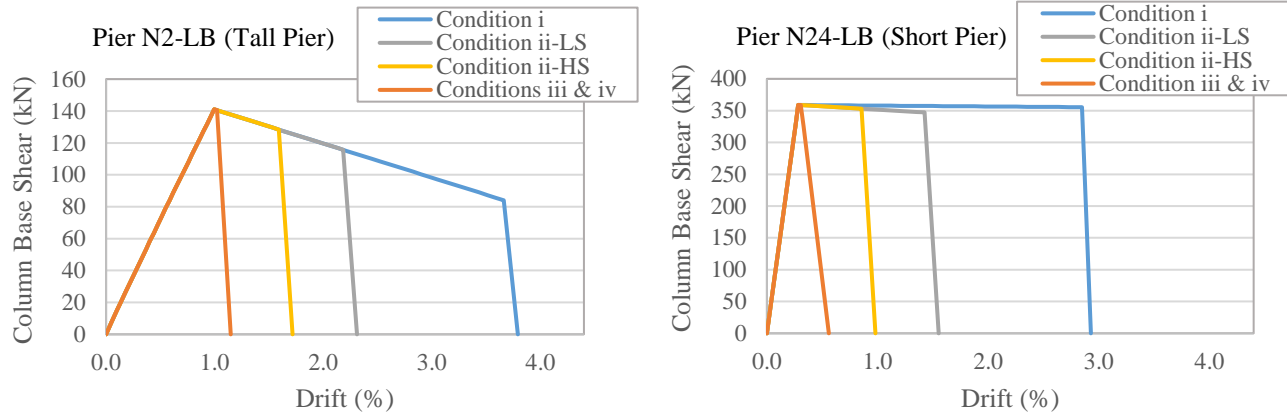


Figure 5. Pushover curves for Pier N2 and N24 models utilizing the lower-bound plastic hinge length

Table 7. Strain limits and curvature ductilities corresponding to the failure of the ASCE 41 hinges

Pier N2-LB ($L_p=0.392$ m)					
	ϵ_c	ϵ_s	φ (rad/m)	φ_e (rad/m)	μ_φ
i	-0.023	0.060	0.071	0.002	40
ii-LS	-0.003	0.035	0.033	0.002	18
ii-HS	-0.002	0.018	0.017	0.002	10
iii	-0.001	0.010	0.010	0.002	5
iv	-0.001	0.010	0.010	0.002	5

Pier N2-UB ($L_p=1.515$ m)					
	ϵ_c	ϵ_s	φ (rad/m)	φ_e (rad/m)	μ_φ
i	-0.002	0.021	0.020	0.002	10
ii-LS	-0.001	0.010	0.010	0.002	5
ii-HS	-0.001	0.006	0.006	0.002	3
iii	-0.001	0.006	0.006	0.002	3
iv	-0.001	0.005	0.005	0.002	3

Pier N24-LB ($L_p=0.392$ m)					
	ϵ_c	ϵ_s	φ (rad/m)	φ_e (rad/m)	μ_φ
i	-0.009	0.074	0.071	0.003	25
ii-LS	-0.003	0.036	0.033	0.003	12
ii-HS	-0.002	0.019	0.018	0.003	6
iii	-0.001	0.004	0.004	0.003	2
iv	-0.001	0.004	0.004	0.003	2